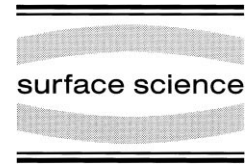




ELSEVIER

Surface Science 454–456 (2000) 880–884



www.elsevier.nl/locate/susc

Brillouin light scattering study of an exchange coupled asymmetric trilayer of Fe/Cr

P. Vavassori ^{a,*}, M. Grimsditch ^b, E. Fullerton ^c, L. Giovannini ^a, R. Zivieri ^a,
F. Nizzoli ^a

^a *INFM-Dipartimento di Fisica, Università di Ferrara, Ferrara I-44100, Italy*

^b *Material Science Division, Argonne National Laboratory, Argonne, IL 60439-4845, USA*

^c *IBM Almaden Research Center, San Jose, CA 95120-6099, USA*

Abstract

The magnetic response of a (211) oriented asymmetric Fe trilayer [Fe(100 Å)/Cr(9 Å)/Fe(20 Å)/Cr(20 Å)/Fe(20 Å)], in which the thickness of the Cr spacer layers was chosen to produce ferromagnetic coupling (F) between the two thinner Fe layers and antiferromagnetic coupling (AF) between the thicker Fe layer and the adjacent thin one, has been investigated using magnetization and Brillouin light scattering (BLS) measurements. The coupling coefficients, extracted by fitting the BLS and magnetization measurements with a theory treating the static and dynamic response on an equal footing, produced consistent values of the magnetic parameters. Our results confirm that the theoretical model used in interpreting both static and dynamic properties is valid even in systems in which F and AF coupling of the layers are simultaneously present. The theoretical model has also been extended to include the field dependence of the intensity of the Brillouin peaks. The calculated intensities are compared with the BLS spectra at different applied fields. © 2000 Elsevier Science B.V. All rights reserved.

Keywords: Green's function methods; Iron; Light scattering; Magnetic interfaces; Magnons

The exchange coupling between two ferromagnetic thin metal films through non-magnetic metallic spacer layers is described by bilinear and biquadratic terms (for a recent and complete review of the argument, see e.g. Ref. [1]). The bilinear term of the coupling is Heisenberg-like so that only ferromagnetic or antiferromagnetic coupling between the two ferromagnetic layers is possible. The coupling oscillates periodically between ferromagnetic and antiferromagnetic with increasing spacer-layer thickness and its origin, as

well as the period of its oscillations, is now well understood. The biquadratic term is phenomenological and was introduced to account for the observation that, under certain conditions, the magnetic moments of the two ferromagnetic layers tend to align at 90° with respect to each other. The origin of the biquadratic coupling is quite controversial and has been attributed to a variety of factors such as interface roughness and intrinsic mechanisms [1].

In this paper we use an experimental approach to determine the coupling coefficients based on the fitting of Brillouin light scattering (BLS) and magnetization measurements with a theory treat-

* Corresponding author. Fax: +39-0532-781810.

E-mail address: vavassor@axpfe.fe.infn.it (P. Vavassori)

ing the static and dynamic response on an equal footing. This approach, successfully used in recent investigations [2–4], is here applied to a [Fe(100 Å)/Cr(9 Å)/Fe(20 Å)/Cr(20 Å)/Fe(20 Å)] multilayer in which the magnetic layers have different thickness. The Brillouin cross-section is then calculated, with a procedure which is a generalization to a layered structure of the method of Cochran and Dutcher [5] for a single film. Our model takes into account the scattering processes which involve reflections of the incident and scattered light on any of the interfaces.

The sample was epitaxially grown by d.c. magnetron sputtering on a polished single-crystal MgO(110) substrate using the same procedure outlined for superlattices [6]. A 100 Å Cr(211) layer was grown at 600°C. The substrate was then cooled to 180°C prior to the growth of the Fe/Cr multilayer. The thickness of the Cr interlayers was chosen to show the simultaneous presence of ferromagnetic and antiferromagnetic coupling between the two thinner Fe layers and between the thicker Fe layer and the adjacent thin one, respectively. The complete structure was capped with a 20 Å Cr layer. A calibrated quartz crystal oscillator monitored the thickness of the various layers. Under these conditions the sample grows with Fe[211] along the surface normal and the in-plane $[\bar{1}11]$ and $[0\bar{1}1]$ directions parallel to MgO $[\bar{1}10]$ and $[001]$, respectively. Magnetization studies have shown that the $[\bar{1}11]$ and $[0\bar{1}1]$ directions are the hard and easy axes, respectively.

The magnetization hysteresis loops were measured by SQUID magnetometry. The spin-wave excitations were measured by BLS using 250 mW of 5145 Å radiation from an Ar⁺ laser. The scattered radiation was analyzed with a tandem Fabry–Perot interferometer [7] in 3+2 pass operation. The sample was mounted with its normal along the collection axis and the laser beam was incident at an angle of 54° to the normal. This geometry fixes the magnitude of the wave vector parallel to the surface q_{\parallel} at $0.98 \times 10^5 \text{ cm}^{-1}$. The magnetic field was applied in the plane of the sample parallel to the $[0\bar{1}1]$ direction (easy axis) and perpendicular to the scattering plane, i.e. perpendicular to the wave vector of the magnon. The polarization of the scattered light was analyzed at 90° to the

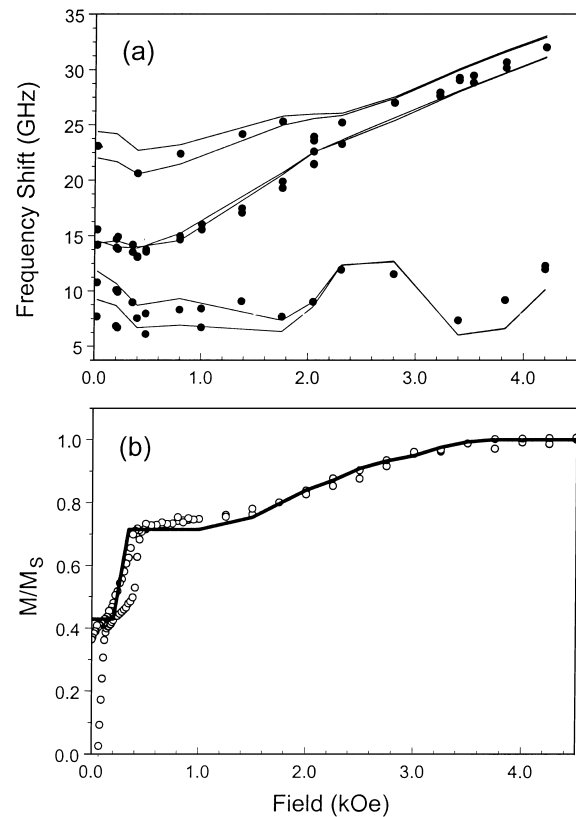


Fig. 1. (a) Brillouin frequencies as a function of the external field applied along the easy axis: experiment (dots) and fit (line) described in the text. (b) Fit (line) of SQUID loop (dots), measured with the field applied along the easy axis, as described in the text.

incident polarization in order to minimize the intense signal of the unshifted laser radiation. All measurements were done at room temperature.

Fig. 1 shows the room temperature magnon frequencies (panel a) and the magnetization results (panel b) of our sample when the external field H is applied along the in-plane easy-axis of the sample. Also shown are the results of the fitting procedure described below. As expected for three magnetic layers, the BLS spectra show three modes: one can be viewed as the in-phase oscillation of the dynamic magnetization m of the three Fe layers and the other two as the out-of-phase oscillation of m of two layers with respect to the third one. The splitting, observed in the calculations at low fields, occurs in the regions where the

Stokes and the anti-Stokes portions of the spectra are not time reversal invariant to each other. For larger fields, where the three layers are aligned with the field, no such differences exist.

The qualitative interpretation of the magnetization curve shows that at low field (0–200 Oe) the static magnetizations M of the two thin Fe layers are parallel to each other, lie in the film plane and are along the easy-axis but antiparallel to H , while M of the thicker layer is parallel to H and thus antiparallel to those of thin layers. In this region $M/M_S = (100 - 20 - 20)/140 = 0.43$, where M_S is the saturation value of M . The magnetization jump observed at $H \gg 300$ Oe is consistent with a switching of the outermost layer so that M of the middle layer is antiparallel to that of the other two layers. Above the jump $M/M_S = (100 - 20 + 20)/140 = 0.71$. A second transition occurring between $H \gg 1$ and 3.5 kOe corresponds to a gradual rotation of M of the central layer till all three layers are aligned; $M/M_S = 1$.

The numerical values of the magnetic parameters have been obtained by fitting the field dependence of the magnetization and BLS results. The basics of the model are described in Ref. [8]; a slightly modified version of that approach was used in Ref. [2]. Our approach here follows Ref. [2]; the energy per layer is unchanged from eq. (1) of Ref. [2]; the total energy per unit area, eq. (2) of Ref. [2], is generalized to three magnetic layers:

$$E = \sum_{i=1}^3 \left\{ K_1 d_i \left(\frac{1}{3} \cos^4 \theta_i + \frac{1}{4} \sin^4 \theta_i \right) + K_u d_i \cos^2 \theta_i - H M_i d_i \cos(\theta_i - \theta_h) \right\} + J_1^{1-2} \cos(\theta_1 - \theta_2) + J_2^{1-2} \cos^2(\theta_1 - \theta_2) + J_1^{2-3} \cos(\theta_2 - \theta_3) + J_2^{2-3} \cos^2(\theta_2 - \theta_3)$$

where K_1 and K_u are the cubic and uniaxial anisotropy constants characteristic of Fe(211) films, M_i is the saturation magnetization of the layer, θ_i and θ_h the angles that M and H make with the hard axis, respectively. The generalization to three layers leads to two bilinear (J_1^{1-2} and J_2^{1-2}) and two biquadratic terms (J_1^{2-3} and J_2^{2-3}). The equilibrium magnetic configuration is calculated minimizing the energy expression above and compared

with the SQUID results. The magnon frequencies are obtained as excited states of the layers above the ground state, generalizing the formalism we used in Ref. [2] to three magnetic layers.

The fitting routine involves adjusting the parameters to produce a minimum in the difference between calculation and experiment (χ^2). The error estimate for each parameter, described in detail in Ref. [2], involves finding the change such that the χ^2 , after adjusting all other parameters, increases by 50%. The best-fit parameters are listed in Table 1 where an asterisk indicates that the fit was insensitive to that particular parameter. (The effects of the cubic anisotropy are small and it is not possible to extract reliable values for K_1 . Therefore we have simply fixed the value of K_1 [2].) During the fitting of the SQUID results we have fixed the values of the anisotropy constants (K_1 and K_u) and of the saturation magnetization in the films (M_1 , M_2 and M_3) to the values extracted from the fits to the BLS data. Fig. 1 shows the good agreement between the experimental data and the fits. A comparison of the results extracted from magnetization and BLS (Table 1) shows that the values of J_1^{i-j} and J_2^{i-j} are within the estimated errors. The model, therefore, provides a self-consistent description of the experimental results even in this case where ferromagnetic and antiferromagnetic coupling is present.

BLS peak intensities were obtained by solving for the eigenmodes of the equations for the dynamic magnetization (eqs. (A5) and (A6) of Ref. [2], generalized to three layers) and the normalization condition requiring that the average energy is the same for each magnon mode. The dynamic magnetization $\mathbf{m}(\mathbf{x}, t)$ induces small fluctuating terms in the dielectric tensor which, to lowest order and for the scattering geometry used here, can be written [9]: $\delta\epsilon_{21} = -Km_3$ and $\delta\epsilon_{23} = Km_1$, where K is the magneto-optic constant. The reference frame, shown in the inset to Fig. 2, has been taken with the x_2 axis along H and the x_3 axis perpendicular to the surface. We have calculated the intensity of the s-polarized scattered light, given a p-polarized incident light, by solving the electromagnetic propagation equation for a stratified medium, which can be written, retaining

Table 1

Table summarizing the parameters extracted from the best least-square fitting of the data shown in Fig. 1. Also shown are confidence levels obtained as described in the text. Asterisks indicate parameters which are fixed during fitting

	K_1 ($\times 10^5$ ergs/ cm^3)	K_u ($\times 10^5$ ergs/ cm^3)	$4\pi M_{1,2}$ (kG)	$4\pi M_3$ (kG)	J_1^{1-2} ($\times 10^{-2}$ ergs/ cm^2)	J_2^{1-2} ($\times 10^{-2}$ ergs/ cm^2)	J_1^{2-3} ($\times 10^{-2}$ ergs/ cm^2)	J_2^{2-3} ($\times 10^{-2}$ ergs/ cm^2)
BLS	1.1*	5.8 ± 0.6	18.0 ± 0.5	17.0 ± 0.8	-8.0 ± 2.5	2.5 ± 2.0	75.0 ± 6.0	15 ± 4.0
SQUID	1.1*	5.8*	18.0*	17.0*	-8.5 ± 2.0	2.5 ± 2.0	72.0 ± 3.0	18 ± 2.0

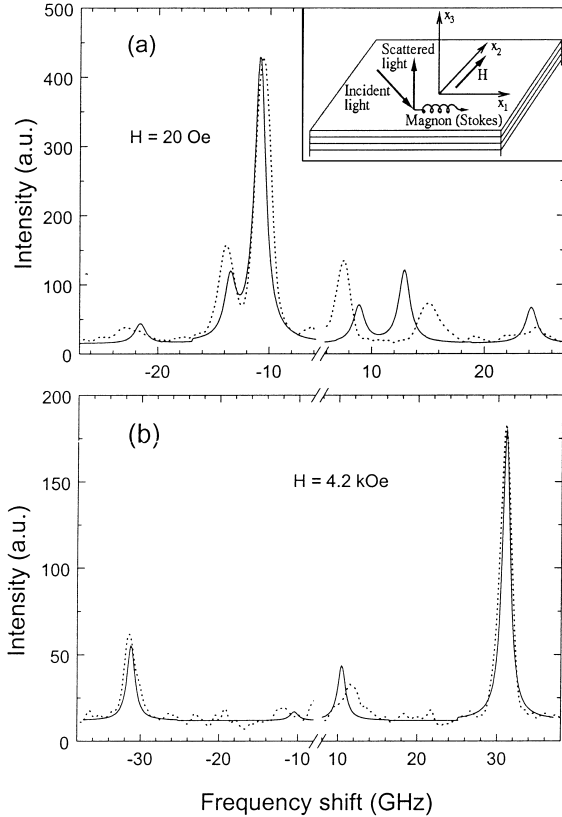


Fig. 2. Comparison between the calculated (solid line) and measured (dashed line) Brillouin spectra at 20 Oe (panel a) and 4.2 kOe (panel b). The inset shows the reference frame used.

the first order fluctuating terms, as

$$\left[\left(-\frac{\omega^2}{c^2} \epsilon_0 + \nabla \times \nabla \times \right) \delta \mathbf{E} \right]_{x_2} = \frac{\omega_0^2}{c^2} (\delta \epsilon_{21} E_1 + \delta \epsilon_{23} E_3).$$

This equation has been solved with the Green’s function method [10], properly taking into account the electromagnetic boundary condition at each interface for the electric field of both incident and scattered light (E and δE , respectively). Finally, the differential Brillouin cross-section is calculated, as the ratio between the scattered intensity and the incident one, times the Bose–Einstein thermal factor. Fig. 2 shows the comparison between the calculated and the measured BLS spectra for $H=20$ Oe (panel a) and $H=4.2$ kOe (panel b). The overall agreement is good; some discrepancies are observed in the anti-Stokes portion of the low field spectrum. The origin of these discrepancies may be due to the critical behavior of the cross-section far from the ferromagnetically aligned state, as already found in the case of the Fe/Cu/Fe system [8]; this issue will be addressed at a later date.

Acknowledgements

Work at ANL was supported by the US Department of Energy, BES under Contract W-31-109-ENG-38. The work of L.G., R.Z. and F.N. has been developed in the framework of the INFM Project SIMBRIS.

References

- [1] S.O. Demokritov, *J. Phys. D: Appl. Phys.* 31 (1998) 925 and references cited therein.
- [2] M. Grimsditch, S. Kumar, E.E. Fullerton, *Phys. Rev. B* 54 (1996) 3385.
- [3] R.J. Hicken, C. Daboo, M. Gester, A.J.R. Ives, S.J. Gray, J.A.C. Bland, *J. Appl. Phys.* 78 (1995) 6670.

- [4] S.M. Rezende, C. Chesman, M.A. Lucena, A. Azevedo, F.M. Aguiar, S.S.P. Parkin, *J. Appl. Phys.* 84 (1998) 958.
- [5] J.F. Cochran, J.R. Dutcher, *J. Magn. Magn. Mater.* 73 (1988) 299.
- [6] E.E. Fullerton, M.J. Conover, J.E. Mattson, C.H. Sowers, S.D. Bader, *Phys. Rev. B* 48 (1993) 15 755.
- [7] J.R. Sandercock, in: M. Cardona, G. Güntherodt (Eds.), *Light Scattering in Solids III*, Springer, Berlin, 1982, p. 173.
- [8] J.F. Cochran, J. Rudd, W.B. Muir, B. Heinrich, Z. Celinski, *Phys. Rev. B* 42 (1990) 508.
- [9] W. Wettleing, M.G. Cottam, J.R. Sandercock, *J. Phys. C* 8 (1975) 211.
- [10] V.I. Smirnov, *A Course of Higher Mathematics Vol. IV* Pergamon, Oxford, 1964.